Distribution and diversity of gallionella-like neutrophilic iron oxidizers in a tidal freshwater marsh

Wang, J.; Vollrath, S.; Behrends, T.; Bodelier, P.L.E.; Muyzer, G.; Den Oudsten, F.; Meima-Franke, M.; Cappellen, P.; Laanbroek, H.J.

published in
Applied and Environmental Microbiology
2011

DOI (link to publisher)
10.1128/AEM.02448-10

document version
Publisher's PDF, also known as Version of record

Applied and Environmental Microbiology, Apr. 2011, p. 2337–2344 Vol. 77, No. 7
0099-2240/11/$12.00 doi:10.1128/AEM.02448-10

Distribution and Diversity of *Gallionella*-Like Neutrophilic Iron Oxidizers in a Tidal Freshwater Marsh▽†‡

Juanjuan Wang,[1]§ Susann Vollrath,[2]§ Thilo Behrends,[2] Paul L. E. Bodelier,[1] Gerard Muyzer,[3] Marion Meima-Franke,[1] Frank Den Oudsten,[1] Philippe Van Cappellen,[2] and Hendrikus J. Laanbroek[1,4]*

Department of Microbial Ecology, Netherlands Institute of Ecology (NIOO-KNAW), Wageningen,[1] Department of Earth Sciences—Geochemistry, Faculty of Geosciences,[2] and Institute of Environmental Biology, Faculty of Science,[4] Utrecht University, Utrecht, and Department of Biotechnology, Environmental Biotechnology Group, Delft University of Technology, Delft,[3] Netherlands

Received 15 October 2010/Accepted 2 February 2011

Microbial iron oxidation is an integral part of the iron redox cycle in wetlands. Nonetheless, relatively little is known about the composition and ecology of iron-oxidizing communities in the soils and sediments of wetlands. In this study, sediment cores were collected across a freshwater tidal marsh in order to characterize the iron-oxidizing bacteria (FeOB) and to link their distributions to the geochemical properties of the sediments. We applied recently designed 16S rRNA primers targeting *Gallionella*-related FeOB by using a nested PCR-denaturing gradient gel electrophoresis (DGGE) approach combined with a novel quantitative PCR (qPCR) assay. *Gallionella*-related FeOB were detected in most of the samples. The diversity and abundance of the putative FeOB were generally higher in the upper 5 to 12 cm of sediment than in deeper sediment and higher in samples collected in April than in those collected in July and October. Oxygen supply by macrofauna appears to be a major force in controlling the spatial and temporal variations in FeOB communities. The higher abundance of *Gallionella*-related FeOB in April coincided with elevated concentrations of extractable Fe(III) in the sediments. Despite this coincidence, the distributions of FeOB did not exhibit a simple relationship to the redox zonation inferred from the geochemical depth profiles.

A characteristic of wetland soils and sediments is the close juxtaposition of oxic and anoxic conditions, which enables intense cycling of carbon, nutrients, and metals (31). The elemental redox cycles are driven by O_2 entering the anoxic zone not only at the sediment surface but also at greater depths, due to O_2 input via aerenchymatous roots of wetland plants and macrofaunal burrows (1, 11, 22). Redox conditions in wetland soils and sediments are highly dynamic because of variations in primary productivity, tidal forcing, temperature, sediment deposition, and groundwater inputs, among others.

As the most abundant transition metal at the Earth's surface, iron (Fe) plays a particularly important role in environmental biogeochemistry (6, 42). Microorganisms can both oxidize and reduce iron. Microbial iron reduction has received abundant attention from both microbiologists and biogeochemists (5, 26). Most work on microbial iron oxidation has focused on acid environments, where competing abiotic oxidation of Fe(II) tends to be negligible (3, 37). Mounting evidence, however, indicates that specialized bacteria are able to oxidize iron under circumneutral pH conditions at oxic-to-anoxic boundaries, where low O_2 concentrations slow down the chemical oxidation of Fe(II) (13, 35). *Gallionella ferruginea* was among the first iron-oxidizing bacteria isolated from this type of environment (16, 39). More recently, Fe-oxidizing bacteria (FeOB) have been detected in various wetland environments (13, 44, 45). A number of isolates have been obtained directly from the rhizosphere of wetland plants (34, 45).

It is becoming increasingly evident that FeOB are ubiquitous in wetland soils and sediments, where they play a major role in the oxidative part of the iron cycle. Nonetheless, our knowledge concerning the distribution and environmental role of neutrophilic iron oxidizers remains rather poor, due in part to the lack of efficient molecular tools for the detection of FeOB. In a previous study, we designed and applied specific primers targeting the 16S rRNA genes of *Gallionella*-like iron-oxidizing bacteria and revealed a much higher diversity in wetland soils than had been known previously (41). The aim of the present study was to delineate the environmental factors, including the presence of plants as well as pore water and solid-phase geochemistry, that influence the distribution and diversity of FeOB in a tidal freshwater marsh.

MATERIALS AND METHODS

Site description and sampling. Sediments were sampled in a tidal freshwater marsh located in the vicinity of the village of Appels, Belgium (5°55′E, 48°46′N), 127 km upstream of the mouth of the Scheldt estuary. The upper marsh is flooded only during exceptionally high tides and is vegetated by willow trees (*Salix alba*), while the lower mudflat is vegetated by bulrushes (*Scirpus lacustris*) and the common reed (*Phragmites australis*) and is flooded twice a day. In between the upper and the lower marsh, the vegetation consists mainly of cattails (*Typha latifolia*). Sediment cores were collected from 3 to 5 locations within the marsh in April, July, and October 2007. The sampling locations were characterized by the absence of vegetation or by the presence of *S. lacustris*, *P. australis*, *T. latifolia*, or *S. alba*. Previous work has shown intense redox cycling of iron in sediments collected in the marsh (20, 24).

* Corresponding author. Mailing address: Department of Microbial Ecology, Netherlands Institute of Ecology (NIOO-KNAW), P.O. Box 50, 6700 AB, Wageningen, Netherlands. Phone: 31-317473400. Fax: 31-317473675. E-mail: r.laanbroek@nioo.knaw.nl.

§ J.W. and S.V. contributed equally to this study.

‡ Publication 5002 of the Netherlands Institute of Ecology.

† Supplemental material for this article may be found at http://aem.asm.org/.

▽ Published ahead of print on 11 February 2011.

In April, all five locations were sampled using Perspex (acrylic glass) tubes with a diameter of 7.6 cm and a length of 35 cm. The tubes were closed at the top with rubber stoppers and at the bottom with discs fitting tightly into the tubes. Before the cores were sliced, the rubber stopper was removed. Then the sediment was incrementally pushed upward by moving the disc and was cut at the top of the tube. Cores for iron extraction were sectioned in the field; those for pore water measurement were processed in the laboratory under an argon atmosphere. During transport, cores and samples were kept at 4°C in the dark until processing in order to minimize chemical changes after sampling (15, 30, 38). In July and October, three locations were sampled: a nonvegetated site and *Scirpus* and *Phragmites* sites. The cores were processed in a glove box within 2 days after sampling. Each core was cut at intervals of 1 cm from 0 to 10 cm and in steps of 2 cm until the bottom of the core. Samples for iron extraction were stored under an argon atmosphere, and samples for molecular analysis were freeze-dried.

Pore water and sediment analyses. Pore water was obtained by centrifugation. The supernatant was filtered (with a 0.2-μm-pore-size nylon filter), and the pH was measured. An aliquot of pore water was used to measure alkalinity spectrophotometrically with bromophenol blue (32). The remaining pore water was acidified with concentrated HCl (10 μl ml^{-1}) for subsequent chemical analyses by inductively coupled plasma optical emission spectroscopy (ICP-OES) and ion chromatography.

A method modified from that of Lovley and Phillips (25) was used to determine Fe(II) and Fe(III) levels in amorphous or poorly crystalline iron phases. These phases include amorphous Fe(III) (hydr)oxide, ferrihydrite, schwertmannite, siderite, vivianite, and amorphous FeS, which are completely extracted (32, 40). Aliquots of 0.1 to 0.2 g of wet sediment were added in a glove box to 0.5 mol $liter^{-1}$ HCl for the extraction of Fe(II) and to 0.5 mol $liter^{-1}$ HCl plus 0.25 mol $liter^{-1}$ hydroxyl ammonium chloride for the extraction of Fe(II) and Fe(III). Suspensions were shaken for an hour, and the extract was subsequently separated from the sediment by centrifugation. Iron concentrations were determined spectrophotometrically with ferrozine at 562 nm using standards of $Fe(NH_4)_2(SO_4)_2 \cdot 6H_2O$ in 0.5 mol $liter^{-1}$ HCl. The amount of extractable Fe(III) was calculated as the difference between the amount of the extract obtained with HCl alone [i.e., Fe(II)] and that obtained with HCl plus hydroxyl ammonium [i.e., Fe(II) plus Fe(III)]. Extraction was performed in triplicate or in duplicate.

Water content (weight loss at 105°C) and organic matter content (weight loss between 105°C and 550°C) were determined by thermogravimetric analysis (TGA). Elemental concentrations of the solid fraction were measured by X-ray fluorescence (XRF). Levels of extractable Fe(II) and Fe(III) were expressed as percentages of the total iron concentrations measured by XRF.

DNA extraction and PCR-denaturing gradient gel electrophoresis (DGGE). DNA was extracted by a modification of the DNA isolation procedure of Zhou et al. (48). DNA was purified using the DNA Clean & Concentrator kit (Zymo Research). The quantity and quality of the extracted DNA were analyzed by spectrophotometry using an ND-1000 spectrophotometer (NanoDrop Technologies, Wilmington, DE) and by agarose gel electrophoresis. The genomic DNA was stored at −20°C for future use.

In the nested PCR-DGGE approach, 16S rRNA genes were first amplified using the newly designed *Gallionella*-specific primer set 122F/998R (41), followed by nested PCR using the primer set 357F/GC907R, specific for bacteria in general (28). One microliter of a 50-ng μl^{-1} soil DNA template was used for a 50-μl PCR volume for each sample. The final PCR products were separated by DGGE, and the representative bands were excised and sequenced.

qPCR. Quantitative PCR (qPCR) primers targeting the 16S rRNA gene of iron-oxidizing bacteria were designed based on known specific primers and probes developed for *Gallionella*-related bacteria. The primer set includes a degenerate forward primer, 628F (GBMAGGCTAGAGTGTAGC), and the reverse primer 998R, which has been used previously in conventional PCR (41). Primers were then compared via a BLAST search and were also compared with the RDP II and ARB databases using the Probe Match function (9, 27) to ascertain primer specificity. The primer pairs were also analyzed for dimer formation by using Primer Premier (Premier Biosoft).

Conventional gradient PCR (55 to 67°C) was performed to test the specificity of the primers and to optimize the annealing temperature. The PCR conditions were as follows: 1 cycle at 95°C for 4 min; 40 cycles of 94°C for 45 s, 55 to 67°C for 20 s, and 72°C for 45 s; and 1 cycle at 72°C for 5 min. The PCR products were checked on a 1% agarose gel in 0.5× Tris-borate-EDTA (TBE) buffer. Based on the position and intensity of the bands, 56°C was chosen as the annealing temperature.

Real-time detection was performed in a 25-μl reaction volume containing 2.5 μl DNA and 22.5 μl SYBR green PCR Master Mix (Invitrogen); 5 pmol μl^{-1} primers and 10 ng μl^{-1} purified environmental DNA were used. PCR was run in 45 cycles, with 1 cycle consisting of denaturation at 95°C for 20 s, annealing at 56°C for 20 s, and extension at 72°C for 45 s. Data were acquired at 82°C for 10 s in order to avoid signals from primer dimer formation. Samples were regarded as being above the detection limit only when a PCR product of the correct size was obtained on an agarose gel after a qPCR run was completed. Each sample was run in duplicate.

Clone MWE_N34, which was used to design the primers, served as a positive control to generate standard curves. The dilution series were made to construct a standard regression line by plotting the cycle threshold (C_T) values versus the logarithm of the starting DNA concentration. Negative controls consisted of clones selected from a clone library described previously (41) (MWE_N10, MWE_C10, MWE_C7, MWE_C36, MWE_N19, MWE_C15, MWE_N10) that are distantly related to the target sequences. The plasmid DNA of the clones was amplified using M13 primers (19), purified, and diluted to serial concentrations in duplicate. The DNA copy number of iron-oxidizing bacteria in each sample was estimated by comparing the C_T value of each sample to the C_T values of the standard regression line. qPCR amplification products were analyzed by electrophoresis in an agarose gel in 0.5× TBE buffer to check for the specificity of the amplification. Sequences were aligned, and phylogenetic trees were constructed with ARB (27, 29) using the neighbor-joining algorithm (http://www.arb-home.de/).

Data analysis. DGGE gels were analyzed using Phoretix gel analysis software (Phoretix International, Newcastle upon Tyne, United Kingdom). The number of bands in each lane was defined, and a matrix of band intensity was created. Lanes were created manually, with a fixed width of 5% of the standard lane width. Each lane represents one sample. Background noise was subtracted by using the rolling-ball algorithm with a radius of 50 pixels. Bands were detected automatically with a minimum slope of 100 and a noise reduction of 4. The bands were then assessed and corrected visually, matched to the reference lane (markers), and quantified. The relative abundance of each band was defined as the ratio of its intensity to the total intensity of the individual lanes for each sample.

A similarity matrix (Bray-Curtis coefficient) was created to assess the similarity in patterns among sites and sampling times. The data were ordinated by nonmetric multidimensional scaling (NMDS; 10 restarts) and cluster analyses with PRIMER software (version 5.2.6; PRIMER-E Ltd., Plymouth, United Kingdom). The differences among the samples were evaluated by the one-way ANOSIM method (analysis of similarities; 999 permutations). Note that the stability index R describes the extent of similarity between each pair in the ANOSIM, with values close to unity indicating that the two groups are entirely separate and a value of zero indicating that there is no difference between the groups.

To correlate environmental variables with the community composition of iron-oxidizing bacteria, the BVSTEP (7) procedure was used (Bray-Curtis similarity coefficient, Spearman rank correlation method; ρ, >0.95; $\Delta\rho$, <0.001). A similarity matrix was first generated for both biological and environmental data; subsequently, a pairwise rank correlation was executed on that matrix. Moreover, a correlation matrix of the biological and environmental data set was created (Statistica, version 9; StatSoft, Inc., Tulsa, OK) to check for possible correlations between different variables.

RESULTS

Sediment and pore water characteristics. The sediments of the tidal marsh were rich in organic matter, with concentrations as high as 10% (wt/wt). Sediment porosity generally decreased with depth (Fig. 1). The porosity gradients, however, were irregular, with local minima and maxima reflecting variations in sediment texture. The local porosity minima correlated with higher solid-phase silicon concentrations (Fig. 1), indicating the presence of coarser, sandy sediment layers. The pore water pH was around 7.5 and did not vary systematically with depth, location, or sampling time. In April, when new roots were not yet well developed and the below-ground biomass was composed mainly of decaying old roots, orange-brown coatings were visually observed around burrow tubes down to a depth of 12 cm below the sediment surface.

Pore water profiles indicated ongoing Fe(III) and SO_4^{2-} reduction in all the sediments (Fig. 1). Build-up of dissolved Fe(II) was typically already detected in the topmost sediment

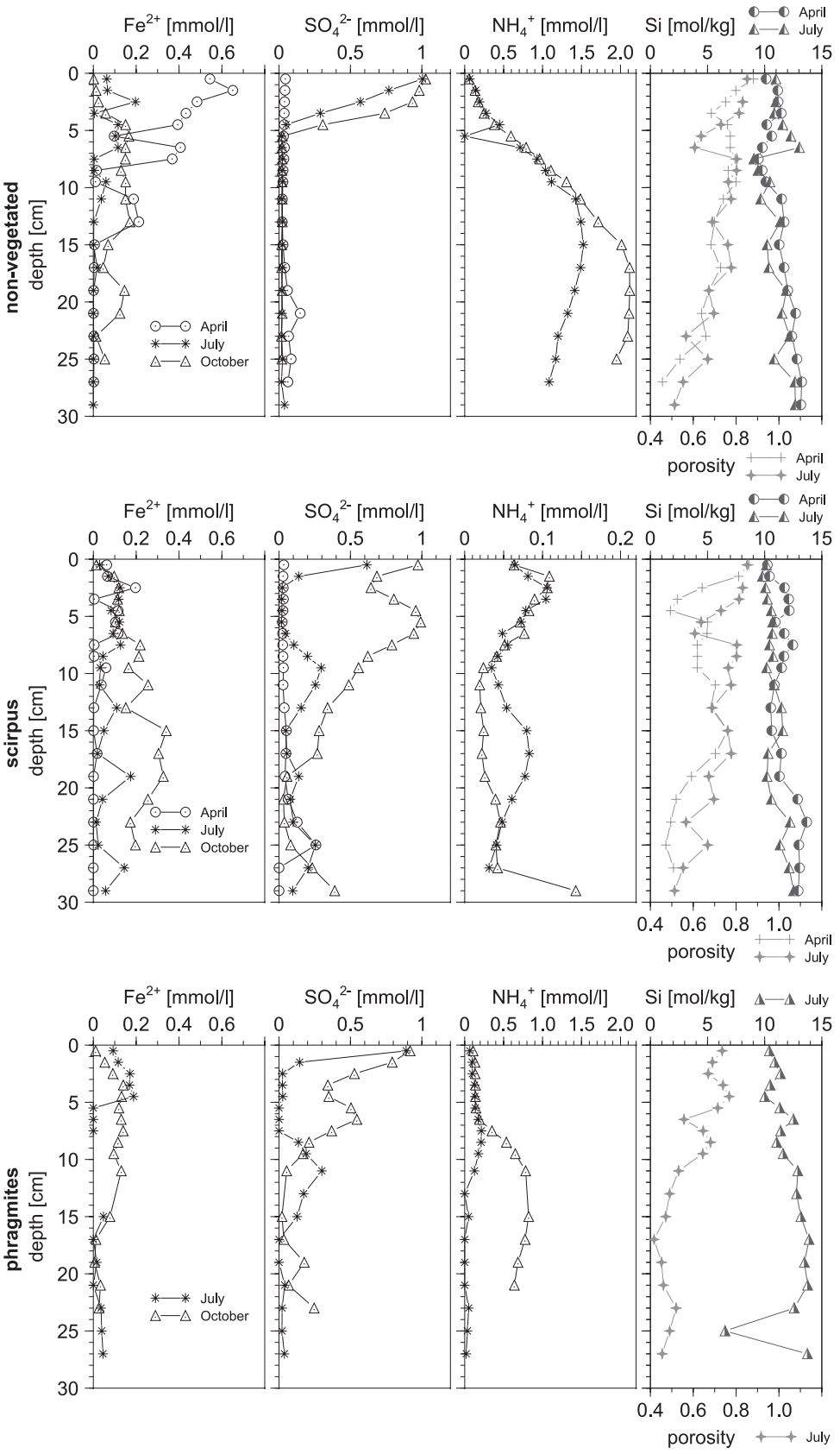

FIG. 1. Examples of vertical profiles of pore water-dissolved iron, sulfate, and ammonium, porosity, and solid-phase silicon collected in April, July, and October. The top, middle, and bottom panels correspond to the nonvegetated, *Scirpus lacustris*, and *Phragmites australis* sites, respectively.

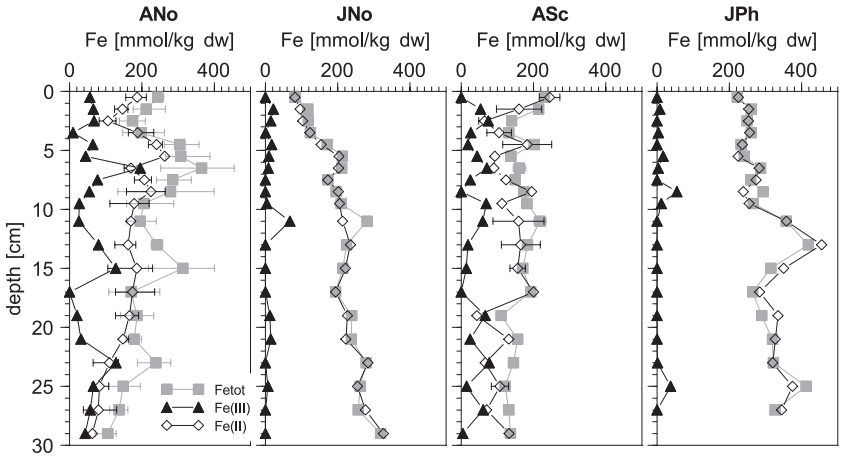

FIG. 2. Depth distributions of total, ferric, and ferrous extractable iron at the different locations sampled in April and July. A, April; J, July; No, nonvegetated; Sc, *Scirpus lacustris*; Ph, *Phragmites australis*. Fe_{tot} is the total concentration of extractable iron, calculated as Fe(II) + Fe(III). Error bars correspond to the standard deviations of measured Fe_{tot} and Fe(II) concentrations in replicate extractions. For the sake of clarity, error bars are not shown for the calculated Fe(III) concentrations.

layers. Pore water sulfate gradients suggested sulfate reduction in the upper 5 to 20 cm of the sediments. High pore water alkalinities (5.7 to 15.7 meq liter^{-1}) were consistent with a dominance of anaerobic respiration processes. The presence and type of vegetation had a marked influence on the pore water profiles. The steepest pore water gradients were observed at the nonvegetated location. At the location with *Scirpus* vegetation, the NH_4^+ concentrations were 15 to 20 times lower than those at the nonvegetated location. The July and October sulfate profiles exhibited a subsurface maximum at the two vegetated locations. No such subsurface maximum was detected at the nonvegetated location.

Extracted iron from amorphous and poorly crystalline phases was present mainly as Fe(II) (Fig. 2). Extractable Fe(III) was detected only in April. Note that measurable Fe(III) concentrations were observed down to the bottom of the cores collected in April. The highest extractable Fe(III) concentrations were found at the nonvegetated location. Comparison of the concentrations of extracted iron and total iron as measured by XRF implied different iron reactivities at the three locations. At the *Phragmites* location, 80 to 100% of total iron was extractable below a depth of 11 cm. At the nonvegetated and *Scirpus* locations, only around 30% of total iron was extractable (data not shown).

FeOB abundance. DNA from *Gallionella*-related iron-oxidizing bacteria was detected by qPCR only in about half the soil samples collected in April, and in none of the samples from July and October (Fig. 3). The total numbers of 16S rRNA gene copies of iron-oxidizing bacteria from July and October were below the detection limit and thus are not shown. The copy numbers ranged from 3.2×10^1 to 7.87×10^5, with a detection limit of 10 copy numbers. The highest copy number was found in the surface layer (0 to 1 cm) of sediment from the *Phragmites* site in April, though only one of the two samples gave products for this site. Most gene copies were detected in samples from the nonvegetated and *Scirpus* locations in April, with a general tendency toward decreasing copy numbers with increasing depth.

FeOB species community composition. DGGE analyses suggested differences in FeOB community composition between the different sites, as well as with depth (see Fig. S1 in the supplemental material). This was especially pronounced in the sediment samples collected in April (see Fig. S1a and b in the supplemental material). Generally speaking, band patterns for the *Phragmites* and *Typha* sites were similar in the April samples and exhibited the highest numbers and relative abundances of bands. The nonvegetated and *Scirpus* sites also showed similar patterns. At each site, the FeOB communities varied with depth. For example, at the nonvegetated, *Scirpus*, and *Phragmites* sites, band 1 disappeared in the two deepest sediment samples, while a different band (band 2B) became present. The latter band was dominant at the *Phragmites* and *Typha* sites (see Fig. S1a and b in the supplemental material). Only a couple of bands were retrieved from the core collected at the *Salix* location, which is seldom exposed to flooding (data not shown).

Fewer bands were detected in July than in April (see Fig. S1a to c in the supplemental material). The relative intensities of the bands also differed at different sampling times. For example, band 3 was the most dominant band at the nonvegetated and *Scirpus* sites in July, while in April, band 1 was dominant at these sites. In October (see Fig. S1d in the supplemental material), even fewer bands were detected than at the other two sampling times. Three weak bands were detected at different depths in the nonvegetated zone, while only one band was expressed in the top layers of sediment at the *Scirpus* and *Phragmites* sites.

In total, four of the six bands were successfully sequenced. Among these, bands 2B and 3 were closely related to *Gallionella ferruginea* (Fig. 4), while bands 1 and 4 were related to sequences of uncultured bacteria, possibly representing unknown iron oxidizers.

Similarities between the compositions of FeOB communities at different times are presented in the NMDS plot (Fig. 5). ANOSIM revealed no significant differences among sites when the results from all sampling times and depths were combined,

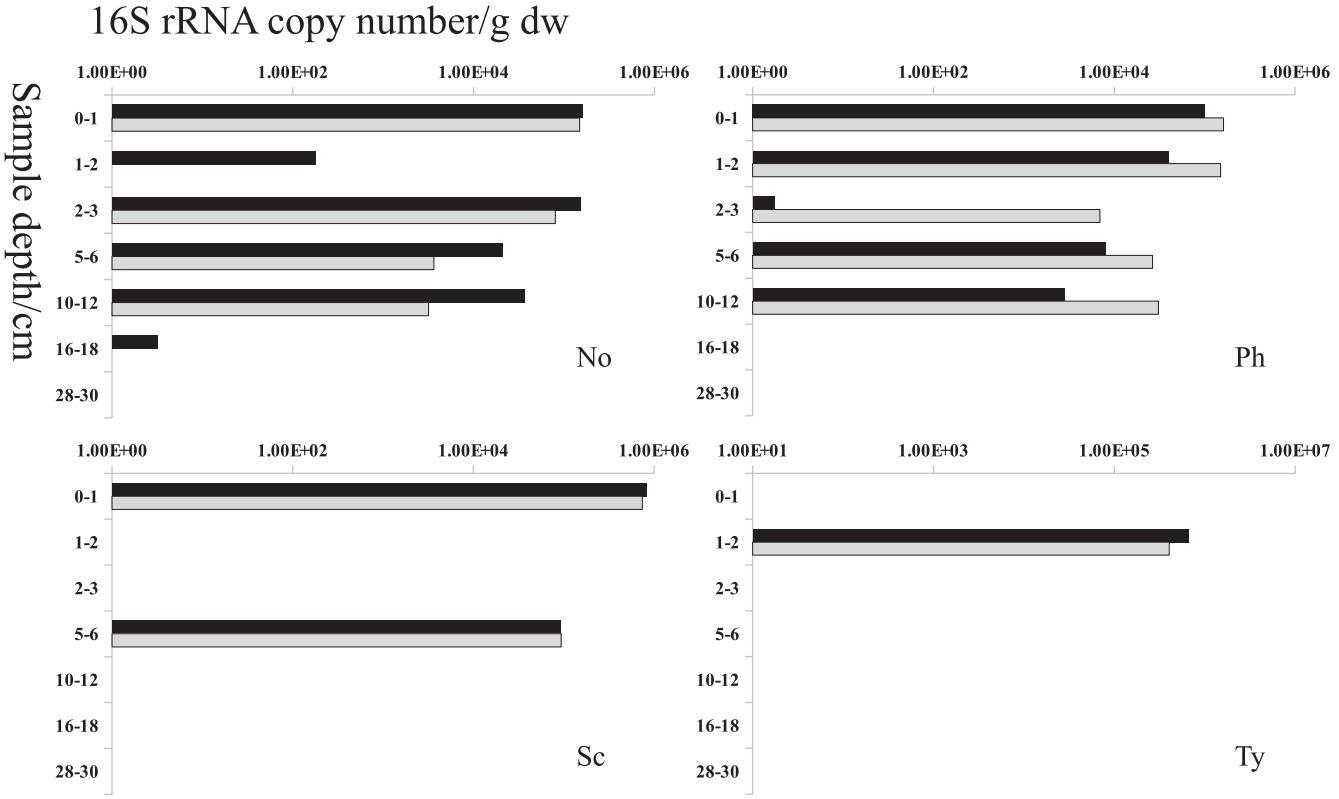

FIG. 3. Abundances of 16S rRNA gene copy numbers from *Gallionella*-related FeOB in samples from different locations of the tidal freshwater marsh collected in April as assessed using a qPCR assay. Duplicates are shown as filled and shaded bars. Samples taken in July and October that were tested by qPCR were below the detection limit and thus are not shown. No, nonvegetated; Sc, *Scirpus lacustris*; Ph, *Phragmites australis*; Ty, *Typha latifolia.*

or among depths when the results from all sites were combined. However, significant differences were observed between the sampling times. Iron-oxidizing bacterial communities were significantly dissimilar between April and July ($R = 0.604$; $P = 0.001$), and between July and October ($R = 0.577$; $P = 0.001$). The differences between April and October were not significant.

Correlation of 16S rRNA data with environmental variables. The BVSTEP analysis showed that, among the different extractable chemical elements, Fe(III) was the most influential factor (ρ, 0.314). Additionally, the nonpairwise correlation results showed that the relative abundance of band 1 was significantly correlated with solid-phase extractable Fe(III) (r^2, 0.5054). Interestingly, the total copy number of 16S rRNA genes was also positively correlated with the relative abundance of band 1 (r^2, 0.41).

DISCUSSION

Our results are consistent with previous studies suggesting that neutrophilic FeOB are widely distributed in wetland soils and sediment. The DGGE analyses demonstrate the presence of several *Gallionella*-like species in the freshwater marsh sediments (14, 17, 21, 43). ANOSIM further suggests significant differences in the abundance and composition of the *Gallionella*-related community from one sampling time to another. This is not entirely unexpected, because the freshwater estuarine environment from which the sediment cores were collected exhibits large seasonal changes in freshwater discharge, tidal forcing, temperature, biological productivity, and supply of allochthonous organic matter (2, 46).

The highest diversity and abundance of putative FeOB, as determined by PCR-DGGE and qPCR, respectively, were observed in the cores collected in April. Among the *Gallionella*-related sequences, band 1 is most pronounced in the DGGE pattern. The relative intensity of this band correlates roughly with the extractable Fe(III) concentrations ($y = 8.58 + 48.10x$; $r^2 = 0.51$) and with the visual presence of Fe(III)-enriched coatings along burrows. Although the number of sampling times in the present study is limited, it would appear that iron-oxidizing bacteria flourish during the spring, leading to localized accumulations of Fe(III) mineral phases in the sediments. The highest number of 16S rRNA gene copies measured is around 8×10^5 per g of soil, indicating an FeOB density comparable to direct cell counts of 10^5 to 10^6 per g of soil reported for wetland soils and bacterial mats (13).

Enhanced iron-oxidizing activity in anoxic sediments during the spring has been reported by Sundby et al. (36), who ascribed it to an enhanced oxygen supply from growing roots. Oxygen availability in the rhizosphere is known to differ both temporally (e.g., diurnal and seasonal fluctuations) and spatially along root systems (43). However, no above-ground parts or novel roots of *Scirpus* plants were observed yet during the

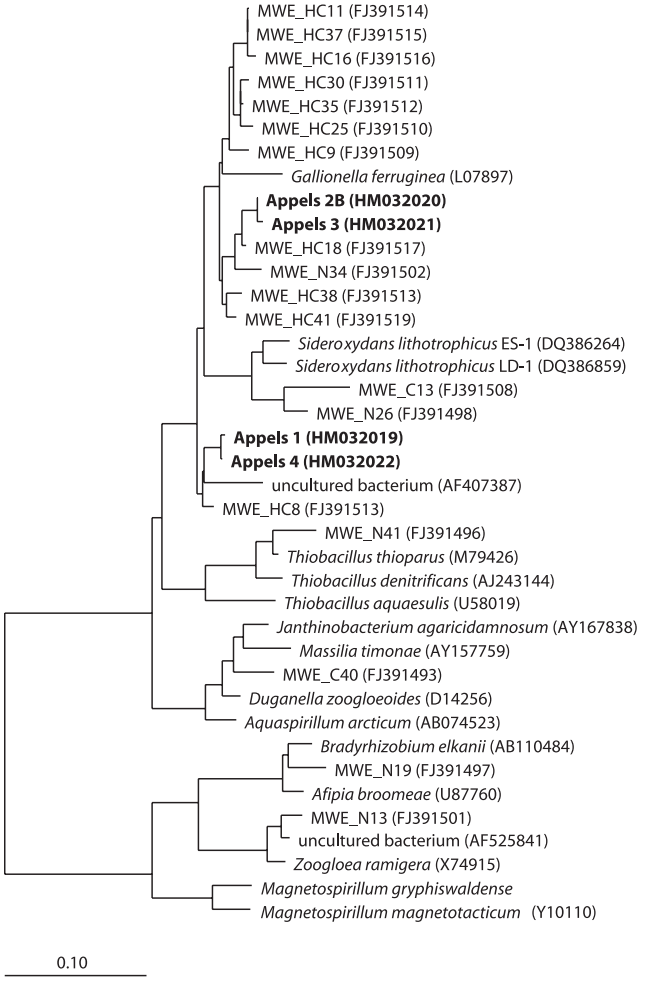

FIG. 4. Phylogenetic tree of *Gallionella*-like partial 16S rRNA gene sequences of DGGE bands (boldface) as well as of cloned sequences (MWE codes) obtained from enrichments in gradient tubes (41). The bar indicates 10% sequence difference.

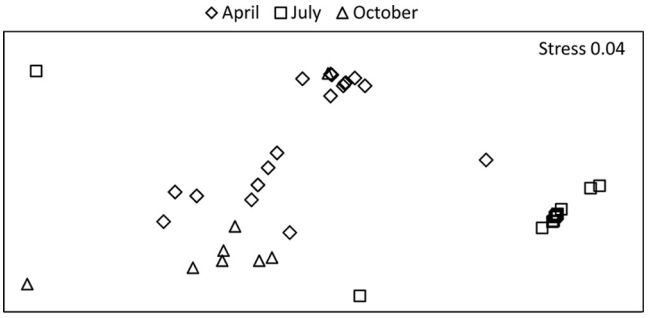

FIG. 5. Ordination by nonmetric multidimensional scaling of $\log(x + 1)$-transformed relative species abundances of the samples taken from nonvegetated, *Scirpus lacustris*, and *Phragmites australis* sites in April, July, and October.

sampling tour in April. Hence, an oxidized rhizosphere could not have been the reason for the higher abundance of *Gallionella*-like species observed at this vegetated site. In addition, similar trends in the depth distribution of 16S rRNA gene copy numbers in the nonvegetated and *Scirpus* sites also point to the absence of oxygen-releasing activities in the rhizosphere of the latter plant species in April. The high abundance of FeOB in both sediments could be stimulated by the growth of macrobenthos during the spring months, which enhances macrofaunal introduction of oxygen into the otherwise anoxic zones of the sediment (4). The nonvegetated mudflat sediments, as well as the *Scirpus* location at the Appels site, are characterized by abundant macrofauna, mainly oligochaete worms (33). Active flushing of macrofaunal burrows introduces oxygenated water well below the depth to which molecular diffusion can resupply oxygen from the overlying water (22). The presence of active ammonia-oxidizing bacteria down to depths of about 10 cm in nonvegetated intertidal sediments from the same Appels site has been linked to vertical mixing of pore water by worms (8).

An additional factor that may help explain the high abundance of putative FeOB in April is temperature. Heinzel et al. (18) reported high microbial iron oxidation rates at relatively low temperatures. Thus, enhanced oxygen supply, through the aerenchyma systems of plants or via vertical mixing by macrofaunal burrows, combined with lower temperatures may create more-favorable conditions for FeOB in the spring than in the summer.

The highest numbers of *Gallionella*-related bacteria are found in the upper 5 to 12 cm of the sediments, that is, the zone where root and macrofaunal activities most strongly impact local redox conditions. At the nonvegetated and *Scirpus* locations, a noticeable change in the composition of the community of *Gallionella*-related bacteria is also observed between the upper and lower sections of the sediment cores. Although the results point to more diverse and abundant FeOB populations in the upper portions of the sediments, they nevertheless imply that FeOB are present at depths where the geochemical profiles indicate globally anoxic conditions (Fig. 1). Koretsky et al. (22) similarly reported the persistence of viable aerobic bacteria at depths well within the sulfidic zone of salt marsh sediments.

Overall, the distributions of FeOB within the Appels marsh sediments exhibit high spatial and temporal heterogeneity. Yu and colleagues also found large changes in the phylogenetic diversity of iron-oxidizing bacteria across short vertical distances at a contaminated aquifer site (47). When the vegetation type and the distribution of the *Gallionella*-related communities are integrated over all sampling times and depths, however, no statistically significant relationship emerges between them, except for the near-absence of detectable FeOB in sediments from the *Salix*-vegetated marsh. Similarly, the community composition of chemolithotrophic ammonia-oxidizing betaproteobacteria in the same tidal freshwater marsh appears to be related not to the presence or type of plants but rather to the elevation within the marsh (23). We speculate that differences in the pattern of flooding between the upper and lower portions of the marsh could be a primary force in iron redox cycling in the sediments and, consequently, in the presence and structure of FeOB communities. Closer correlations between geochemistry and microbial communities may possibly be found at small spatial scales on the order of millimeters or below. This would require the application of microbial and analytical techniques with high spatial resolution (10, 12). Additionally, the inclusion in the survey of primer sets for other iron-oxidizing organisms might help to better constrain the

connection between physical and chemical conditions and the iron-oxidizing activity in wetlands.

In conclusion, *Gallionella*-related FeOB inhabit vegetated and nonvegetated sediments of the tidal marsh at Appels in the upper freshwater part of the Scheldt estuary. Cell densities range from below detection to 10^6 cells per g of sediment. Thus, together with previous studies, our results support a widespread distribution of neutrophilic, putative FeOB in wetland soils and sediments. Although several FeOB species are present in the sediments of the Appels marsh, one dominant species appears to be closely associated with the abundance of reactive Fe(III) phases. The highest diversity and abundance of the FeOB are found in the upper 5 to 12 cm of the sediments retrieved in April, probably due to enhanced root and macrofaunal activity during the spring season. However, the composition and abundance of the *Gallionella*-related FeOB do not exhibit otherwise straightforward relationships with the geochemical conditions in the sediments. The lack of simple correlations between geochemistry and microbial communities is probably common in marsh sediments (22).

ACKNOWLEDGMENT

This work was financially supported by the Netherlands Darwin Center for Biogeology (grants 142.16.1031 and 142.16.1032).

REFERENCES

1. **Armstrong, W.** 1964. Oxygen diffusion from roots of some British bog plants. Nature **204:**801. (Letter.)
2. **Baeyens, W., B. van Eck, C. Lambert, R. Wollast, and L. Goeyens.** 1998. General description of the Scheldt estuary. Hydrobiologia **366:**1–14.
3. **Baker, B. J., and J. F. Banfield.** 2003. Microbial communities in acid mine drainage. FEMS Microbiol. Ecol. **44:**139–152.
4. **Beukema, J. J.** 1974. Seasonal changes in the biomass of the macro-benthos of a tidal flat area in the Dutch Wadden Sea. Netherlands J. Sea Res. **8:**94–107.
5. **Bonneville, S., T. Behrends, and P. Van Cappellen.** 2009. Solubility and dissimilatory reduction kinetics of iron(III) oxyhydroxides: a linear free energy relationship. Geochim. Cosmochim. Acta **73:**5273–5282.
6. **Borch, T., et al.** 2010. Biogeochemical redox processes and their impact on contaminant dynamics. Environ. Sci. Technol. **44:**15–23.
7. **Clarke, K. R., and R. M. Warwick.** 1998. Quantifying structural redundancy in ecological communities. Oecologia **113:**278–289.
8. **Coci, M., et al.** 2005. Effect of salinity on temporal and spatial dynamics of ammonia-oxidising bacteria from intertidal freshwater sediment. FEMS Microbiol. Ecol. **53:**359–368.
9. **Cole, J. R., et al.** 2005. The Ribosomal Database Project (RDP-II): sequences and tools for high-throughput rRNA analysis. Nucleic Acids Res. **33:**D294–D296.
10. **Dechesne, A., et al.** 2003. A novel method for characterizing the microscale 3D spatial distribution of bacteria in soil. Soil Biol. Biochem. **35:**1537–1546.
11. **Doyle, M. O., and M. L. Otte.** 1997. Organism-induced accumulation of iron, zinc and arsenic in wetland soils. Environ. Pollut. **96:**1–11.
12. **Druschel, G. K., D. Emerson, R. Sutka, P. Suchecki, and G. W. Luther.** 2008. Low-oxygen and chemical kinetic constraints on the geochemical niche of neutrophilic iron(II) oxidizing microorganisms. Geochim. Cosmochim. Acta **72:**3358–3370.
13. **Emerson, D., and C. Moyer.** 1997. Isolation and characterization of novel iron-oxidizing bacteria that grow at circumneutral pH. Appl. Environ. Microbiol. **63:**4784–4792.
14. **Emerson, D., and N. P. Revsbech.** 1994. Investigation of an iron-oxidizing microbial mat community located near Aarhus, Denmark—field studies. Appl. Environ. Microbiol. **60:**4022–4031.
15. **Förstner, U.** 2004. Traceability of sediment analysis. Trends Anal. Chem. **23:**217–236.
16. **Hallbeck, L., and K. Pedersen.** 1990. Culture parameters regulating stalk formation and growth-rate of *Gallionella ferruginea*. J. Gen. Microbiol. **136:** 1675–1680.
17. **Hanert, H. H.** 2002. Bacterial and chemical iron oxide deposition in a shallow bay on Palaea Kameni, Santorini, Greece: microscopy, electron probe microanalysis, and photometry of in situ experiments. Geomicrobiol. J. **19:**317–342.
18. **Heinzel, E., E. Janneck, F. Glombitza, M. Schlomann, and J. Seifert.** 2009. Population dynamics of iron-oxidizing communities in pilot plants for the treatment of acid mine waters. Environ. Sci. Technol. **43:**6138–6144.
19. **Huey, B., and J. Hall.** 1989. Hypervariable DNA fingerprinting in *Escherichia coli*: minisatellite probe from bacteriophage M13. J. Bacteriol. **171:**2528–2532.
20. **Hyacinthe, C., S. Bonneville, and P. Van Cappellen.** 2006. Reactive iron(III) in sediments: chemical versus microbial extractions. Geochim. Cosmochim. Acta **70:**4166–4180.
21. **James, R. E., and F. G. Ferris.** 2004. Evidence for microbial-mediated iron oxidation at a neutrophilic groundwater spring. Chem. Geol. **212:**301.
22. **Koretsky, C. M., et al.** 2005. Salt marsh pore water geochemistry does not correlate with microbial community structure. Estuar. Coast. Shelf Sci. **62:** 233–251.
23. **Laanbroek, H. J., and A. Speksnijder.** 2008. Niche separation of ammonia-oxidizing bacteria across a tidal freshwater marsh. Environ. Microbiol. **10:** 3017–3025.
24. **Lin, B., et al.** 2007. Phylogenetic and physiological diversity of dissimilatory ferric iron reducers in sediments of the polluted Scheldt estuary, Northwest Europe. Environ. Microbiol. **9:**1956–1968.
25. **Lovley, D. R., and E. J. P. Phillips.** 1987. Rapid assay for microbially reducible ferric iron in aquatic sediments. Appl. Environ. Microbiol. **53:**1536–1540.
26. **Lovley, D. R., E. J. P. Phillips, and D. J. Lonergan.** 1991. Enzymatic versus nonenzymatic mechanisms for Fe(III) reduction in aquatic sediments. Environ. Sci. Technol. **25:**1062–1067.
27. **Ludwig, W., et al.** 2004. ARB: a software environment for sequence data. Nucleic Acids Res. **32:**1363–1371.
28. **Muyzer, G., E. C. Dewaal, and A. G. Uitterlinden.** 1993. Profiling of complex microbial populations by denaturing gradient gel electrophoresis analysis of polymerase chain reaction-amplified genes coding for 16S rRNA. Appl. Environ. Microbiol. **59:**695–700.
29. **Pruesse, E., et al.** 2007. SILVA: a comprehensive online resource for quality checked and aligned ribosomal RNA sequence data compatible with ARB. Nucleic Acids Res. **35:**7188–7196.
30. **Rapin, F., A. Tessier, P. G. C. Campbell, and R. Carignan.** 1986. Potential artifacts in the determination of metal partitioning in sediments by a sequential extraction procedure. Environ. Sci. Technol. **20:**836–840.
31. **Roden, E. E., and R. G. Wetzel.** 1996. Organic carbon oxidation and suppression of methane production by microbial Fe(III) oxide reduction in vegetated and unvegetated freshwater wetland sediments. Limnol. Oceanogr. **41:**1733–1748.
32. **Sarazin, G., G. Michard, and F. Prevot.** 1999. A rapid and accurate spectroscopic method for alkalinity measurements in sea water samples. Water Res. **33:**290–294.
33. **Seys, J., M. Vincx, and P. Meire.** 1999. Spatial distribution of oligochaetes (Clitellata) in the tidal freshwater and brackish parts of the Schelde estuary (Belgium). Hydrobiologia **406:**119–132.
34. **Sobolev, D., and E. E. Roden.** 2004. Characterization of a neutrophilic, chemolithoautotrophic Fe(II)-oxidizing beta-proteobacterium from freshwater wetland sediments. Geomicrobiol. J. **21:**1–10.
35. **Sobolev, D., and E. E. Roden.** 2001. Suboxic deposition of ferric iron by bacteria in opposing gradients of Fe(II) and oxygen at circumneutral pH. Appl. Environ. Microbiol. **67:**1328–1334.
36. **Sundby, B., C. Vale, M. Caetano, and G. W. Luther.** 2003. Redox chemistry in the root zone of a salt marsh sediment in the Tagus Estuary, Portugal. Aquat. Geochem. **9:**257–271.
37. **Tan, G. L., et al.** 2009. Seasonal and spatial variations in microbial community structure and diversity in the acid stream draining across an ongoing surface mining site. FEMS Microbiol. Ecol. **70:**121–129.
38. **Thomson, E. A., S. N. Luoma, D. J. Cain, and C. Johansson.** 1980. The effect of sample storage on the extraction of Cu, Zn, Fe, Mn and organic material from oxidized estuarine sediments. Water Air Soil Pollut. **14:**215–233.
39. **Vatter, A. E., and R. S. Wolfe.** 1956. Electron microscopy of *Gallionella ferruginea*. J. Bacteriol. **72:**248–252.
40. **Wallmann, K., K. Hennies, I. König, W. Petersen, and H. D. Knauth.** 1993. New procedure for determining reactive Fe(III) and Fe(II) minerals in sediments. Limnol. Oceanogr. **38:**1803–1812.
41. **Wang, J. J., G. Muyzer, P. L. E. Bodelier, and H. J. Laanbroek.** 2009. Diversity of iron oxidizers in wetland soils revealed by novel 16S rRNA primers targeting *Gallionella*-related bacteria. ISME J. **3:**715–725.
42. **Weber, K. A., L. A. Achenbach, and J. D. Coates.** 2006. Microorganisms pumping iron: anaerobic microbial iron oxidation and reduction. Nat. Rev. Microbiol. **4:**752–764.
43. **Weiss, J. V., D. Emerson, S. M. Backer, and J. P. Megonigal.** 2003. Enumeration of Fe(II)-oxidizing and Fe(III)-reducing bacteria in the root zone of wetland plants: implications for a rhizosphere iron cycle. Biogeochemistry **64:**77–96.
44. **Weiss, J. V., D. Emerson, and J. P. Megonigal.** 2004. Geochemical control of microbial Fe(III) reduction potential in wetlands: comparison of the rhizosphere to non-rhizosphere soil. FEMS Microbiol. Ecol. **48:**89–100.
45. **Weiss, J. V., et al.** 2007. Characterization of neutrophilic Fe(II)-oxidizing

bacteria isolated from the rhizosphere of wetland plants and description of *Ferritrophicum radicicola* gen. nov. sp. nov., and *Sideroxydans paludicola* sp. nov. Geomicrobiol. J. **24:**559–570.
46. **Wollast, R.** 1988. The Scheldt estuary, p. 183–193. *In* W. Salomons, B. Blayne, E. Duursma, and U. Forstmer (ed.), Pollution of the North Sea: an assessment. Springer-Verlag, Berlin, Germany.
47. **Yu, R., P. Gan, A. A. MacKay, S. L. Zhang, and B. F. Smets.** 2010. Presence, distribution, and diversity of iron-oxidizing bacteria at a landfill leachate-impacted groundwater surface water interface. FEMS Microbiol. Ecol. **71:** 260–271.
48. **Zhou, J. Z., M. A. Bruns, and J. M. Tiedje.** 1996. DNA recovery from soils of diverse composition. Appl. Environ. Microbiol. **62:**316–322.